Available online at www.sciencedirect.com

ScienceDirect

Procedia Engineering 10 (2011) 1991–1996

Engineering Procedia

The cyclic elasto-viscoplastic behavior of a high-speed steel under forging conditions – experiments and simulations

Anton Ishmurzin[a,*], Werner Ecker[a], Martin Krobath[a], Markus Orthaber[a], Stefan Marsoner[a], Thomas Antretter[b]

[a]*Materials Center Leoben Forschung GmbH, Leoben A-8700, Austria*
[b]*Institute for Mechanics, Montanuniversitaet Leoben, Leoben A-8700, Austria*

Abstract

High speed steels are an important material for manufacturing of various cutting tools as well as punches and dies. The modeling of the cyclic behavior of the steels for the use within the finite element framework is of a paramount importance for successful computer-aided engineering of such tools. A successful model for the cyclic behavior of high speed steels should be able to represent a variety of mechanical effects. For the given steel we propose an extended material model based on the ideas of Armstrong-Frederick and Chaboche. The model consists of evolution equations that take into account nonlinear isotropic, nonlinear kinematic and threshold nonlinear kinematic hardening mechanisms. The tension-compression asymmetry is reproduced by incorporating a term proportional to the third stress invariant into the viscoplastic potential. In order to facilitate the modeling of the high speed steel a range of strain-controlled and stress-controlled experiments was carried out. The calibration of a model is performed using an optimization software tool using the experimental data. The simulation capability of the model is illustrated by applying the material model to the cyclic behavior of a forging die.

Selection and peer-review under responsibility of ICM11

Keywords: cyclic plasticity, high strength steel, Armstrong-Frederick, hardening, strength differential effect, cold forging, constitutive model

1. Introduction and Motivation

Typical materials for cold forging tools are cold work tool steels or high speed steels (HSS). The present publication deals with the modeling of the cyclic behavior of a HSS Böhler S390 Microclean [1] at a hardness at 66 HRC in cold forging conditions.

During cold forging, the forging tool undergoes compressive external cyclic loading which causes its plastic deformation. As a result, tensile residual stresses form in such a tool [2]. The

*Corresponding author. Tel.: +43-3842-45922-35; fax: +43-3842-45922-5.
Email address: anton.ishmurzin@mcl.at (Anton Ishmurzin)

1877-7058 © 2011 Published by Elsevier Ltd. Open access under CC BY-NC-ND license.
Selection and peer-review under responsibility of ICM11 doi:10.1016/j.proeng.2011.04.330

mechanism of the residual stresses formation is crucial for the lifetime prediction of forming tools.

There has been extensive improvement in the modeling of the cyclic behavior of metallic alloys, starting with the seminal work of Armstrong and Frederick in 1966 [3], followed by further improvements by Chaboche and Jung [4], which improve the description of ratcheting effects by introducing a "modified recall term with a threshold". The threshold model was successfully applied to describe the cyclic behavior of different materials.

As many other high strength steels, S390 Microclean exhibits an asymmetric behavior in tension and compression, also known as strength differential effect (SDE) [5, 6, 7], which has not been addressed within the framework of Armstrong-Frederick-Chaboche's threshold model. This gap is addressed in the present publication.

In isotropic conditions the yield function f generally depends on three stress invariants I_1, J_2, and J_3. The dependence of the yield function on I_1 for this class of materials is weak and $f(J_2, J_3)$ can be used successfully [5, 8, 9]. In the opinion of the authors, usage of I_1 is not physically justified. The reason is, that I_1 as the trace of the stress tensor corresponds to volume effects. However, high strength steels are not known to exhibit such volume effects. One feasible way to account for the SDE is given in [10], which is also used in the present publication.

In order to calibrate the model, heat-treated steel specimens at a hardness of 66 HRC were subjected to uniaxial cyclic tests with different loading ratios.

The ability of the model to represent the behavior observed in cyclic experiments is discussed.

Furthermore, an exemplary finite element simulation of a cold forging process is presented.

2. Constitutive model

The newly developed constitutive model for high strength steels considering the SDE is described below.

Additivity of the elastic and the plastic parts of the strain tensor is assumed in the small strain framework:

$$\boldsymbol{\epsilon}_\mathrm{t} = \boldsymbol{\epsilon}_\mathrm{e} + \boldsymbol{\epsilon}_\mathrm{p}. \tag{1}$$

The elastic part of the strain is Hookean (linear-elastic)

$$\boldsymbol{\epsilon}_\mathrm{e} = \frac{1+\nu}{E}\boldsymbol{\sigma} - \frac{\nu}{E}(\mathrm{tr}\,\boldsymbol{\sigma})\boldsymbol{I}, \tag{2}$$

where E is the Young's modulus, ν - Poisson's ratio, $\boldsymbol{\sigma}$ - stress tensor and $\boldsymbol{I}$ is the second order unit tensor. The plastic part is defined as

$$\dot{\boldsymbol{\epsilon}}_\mathrm{p} = \dot{\nu}\boldsymbol{n} = \dot{\nu}\frac{\partial f/\partial\boldsymbol{\sigma}}{\|\partial f/\partial\boldsymbol{\sigma}\|}, \tag{3}$$

where $f = f(\boldsymbol{\sigma})$ is the yield function, derived a modified Mises potential accounting for the SDE [10]:

$$f(\boldsymbol{\sigma}) = J_2(\boldsymbol{s}-\boldsymbol{x})\left[1 + a\frac{J_3(\boldsymbol{s}-\boldsymbol{x})}{J_2(\boldsymbol{s}-\boldsymbol{x})^{n/2}}\right] - r, \tag{4}$$

where $\boldsymbol{s}$ is the deviatoric stress tensor, $\boldsymbol{x} = \sum_{i=1}^{i=N}\boldsymbol{x}_i$ is the sum of N backstresses employed in the model, n is a positive natural integer (in this case set to $n = 3$), J_2 and J_3 are the second and the

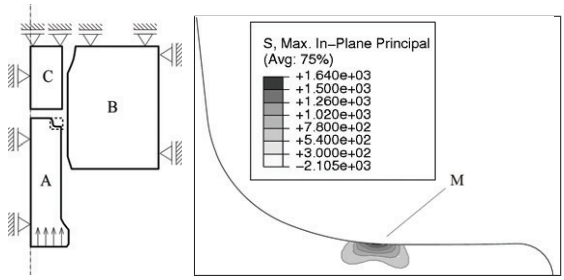

(a) (b)

Figure 1: (a) A schematic representation of the simulated forging process. Part A (S390 Microclean) is the punch, part B (S390 Microclean) is the forging die and the part C (16MnCr5) is the blank. A small rectangle shows the region with highest loading, where point M is chosen. (b) Maximum in-plane stresses around point M.

third deviatoric stress invariants, v is the plastic multiplier, a – an empirical parameter, whose dimension depends the choice of n and $r = \sum_{i=0}^{i=2} r_i$ is the sum of the initial yield stress r_0 and the isotropic hardening functions $r_i = Q_i[1 - \exp(-b_i v)]$, $i = 1, 2$ with Q_i and b_i being material parameters.

Note that the yield function (4) degenerates to the standard von Mises yield function when $a = 0$. Also note that for some combination of the parameters n and a the set $f(\boldsymbol{\sigma}) \leq 0$ is not convex. A way to ensure convexity is described in [11].

The model uses threshold versions of kinematic strain hardening terms as suggested by Chaboche in [12, 4]. A kinematic hardening backstress $\boldsymbol{x_i}$ is assumed to have a corresponding internal variable ("backstrain") $\boldsymbol{\alpha}_i$, defined as $\boldsymbol{x_i} = {}^2/_3 C_i \boldsymbol{\alpha}_i$. The evolution equation for a backstress in terms of $\boldsymbol{\alpha}_i$ is

$$\dot{\boldsymbol{\alpha}}_{\boldsymbol{i}} = \left[\boldsymbol{n} - \frac{3D_i}{2C_i}\boldsymbol{\mathcal{P}}_i : \boldsymbol{x}_i\right]\dot{v},\ \boldsymbol{\mathcal{P}}_i = \left\langle \frac{D_i(\boldsymbol{x_i}) - \omega_i C_i}{1 - \omega_i} \right\rangle \frac{1}{D_i J_2(\boldsymbol{x_i})}\boldsymbol{\mathcal{I}}, \tag{5}$$

where C_i and D_i are empirical parameters, $\boldsymbol{\mathcal{P}}_i$ is a fourth-order tensor, the parameter $0 \leq \omega_i < 1$ describes the transition from linear to nonlinear kinematic hardening and $\boldsymbol{\mathcal{I}}$ is the fourth order unit tensor. Since the steel in question does not exhibit rate-dependent behavior under cold forging conditions, standard rate-independent plasticity is assumed. The model presented is both implemented as UMAT and calibrated, based on uniaxial experimental data by means of the Zebulon software package [13]. Details on such a calibration process can be found in [4].

3. Finite element model

In an axial-symmetric finite element model using the software package Abaqus 6.10 [14] a typical cold forging process is analyzed. The forging tool consists of a die and a punch. For both parts the newly developed constitutive model for the HSS S390 Microclean at a hardness of 66 HRC is used. For the blank a flow curve for 16MnCr5 steel is taken from [15]. A sketch of the model describing the geometry and the boundary conditions is depicted in Fig. 1a.

The process is controlled by a displacement boundary condition at the bottom surface of the punch. Only one loading cycle is computed with the model described in Fig. 1a including contact

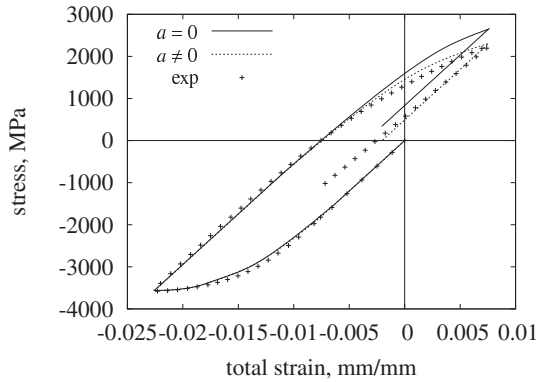

Figure 2: Comparison of stress-strain curves during the first cycle for a one-element test. The marker represents the experimental data, the solid line the simulation without the SDE ($a = 0$), the dotted line the simulation with the SDE taken into account ($a \neq 0$).

between each of the parts A, B and C. For the sake of simplicity and to save computation time, only the punch is modeled in the repeated cycles. The loading of the punch is considered by applying the contact forces taken from the model of the first cycle onto the contact surface of the punch. Using this method, 100 loading cycles are investigated.

4. Results

The constitutive model described above is used to describe the cyclic behavior of S390 Microclean steel of 66 HRC. The parameters of the model are calibrated based on uniaxial cyclic tests. For comparison purposes, the corresponding tension-compression symmetric model is calibrated in the same way.

The presented model taking the SDE into account on one hand and the corresponding symmetrical model ($a = 0$, other parameters optimized anew) on the other hand, are used for single element test simulations in order to be compared with the experimental cyclic test data. The comparison for the first cycle of the test is shown in Fig. 2. In the lower left quadrant where the compression takes place, the figure shows a close agreement between both simulated curves and the experiment. Contrary to that, in the opposite quadrant of the tension, only the curve produced by the proposed constitutive model is in good agreement with the experiment.

The accurate prediction of the development of residual stresses is necessary for successful life time evaluation. In order to illustrate the development of residual stresses, a representative point is chosen (Fig. 1b). This point experiences the highest maximum principal stress due to external loading, one time increment before the punch reaches its highest position, right before its downward motion starts.

The development of the distribution of the residual stress is investigated in the adjacent area of point M. Due to plastic deformation in the compressive stress region near the surface of the punch, tensile residual stresses form during the forging process (Fig. 3). After the first cycle, the maximum residual stress is located near the left end of the punch radius. The residual stress after the first cycle around point M is 22 MPa, whereas the maximum residual stress is 243 MPa. After 100 cycles the situation changes considerably. The residual stress maximum of the first

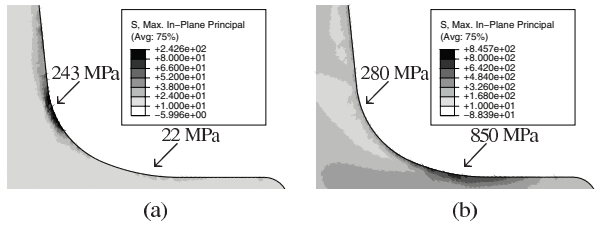

Figure 3: Development of residual stresses in the punch in the zone with highest loading (Fig. 1a) after (a) 1 and (b) 100 cycles.

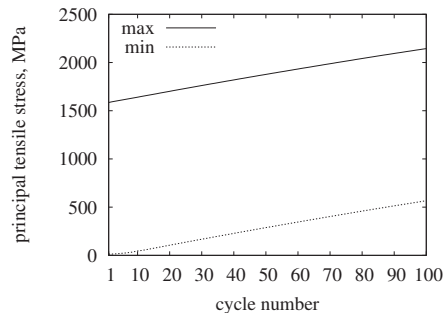

Figure 4: Evolution of minimum and maximum principal tensile stresses at point M.

cycle near the left end of the punch radius remains almost unchanged (280 MPa), whereas the residual stress near point M reaches 850 MPa.

Figure 4 shows the increase of the principal stresses due to the evolution of residual stresses, in the investigated point M. It can be seen that the minimum and the maximum principal stress increase similarly. The stress amplitude $\Delta\sigma$ remains almost constant ($\Delta\sigma_1$ = 1572 MPa and $\Delta\sigma_{100}$ = 1577 MPa), whereas the stress ratio decreases from R_1 = 119.3 to R_{100} = 3.78.

5. Discussion and Conclusions

The constitutive model for representation of the cyclic behavior of high strength steels exhibiting the SDE was derived based on the modification of the yield function found in the literature. The constitutive model was calibrated using uniaxial cyclic test data. Additionally it is planned to investigate the model in multiaxial loading conditions.

The inclusion of the J_3-term into the yield function improves the agreement of single-element cyclic simulation with the cyclic experiment data considerably. The difference between simulated cyclic stress-strain curves with and without the SDE taken into account in the compression area is insignificant: they both agree with the experimental data. On the other hand, during tension, the difference between the two curves increases with the increase of the tensile loading. Thus the proposed constitutive model can be used in the cases where accurate representation of tension is important.

The finite element simulation of a typical forging problem showed that the area near the surface of the tool undergoes local cyclic plastic deformation. The deformation leads to the accu-

mulation of residual stresses. A further investigation of the maximum and minimum stresses revealed that the stress amplitude $\Delta\sigma$ does not change significantly with the cycle number, whereas the stress ratio R increases. An accurate prediction of $\Delta\sigma$ and R provides the basis for life time calculations.

Thus, the proposed finite element simulation of forging tools allows to identify critical areas and to estimate fatigue behavior. Since the underlying constitutive model has a better ability to represent the cyclic material behavior, the overall accuracy of the life time prediction for tools made of high strength steels that exhibit the SDE can be increased.

Acknowledgements

Financial support by the Austrian Federal Government (in particular from the Bundesministerium für Verkehr, Innovation und Technologie and the Bundesministerium für Wirtschaft, Familie und Jugend) and the Styrian Provincial Government, represented by Österreichische Forschungsförderungsgesellschaft mbH and by Steirische Wirtschaftsförderungsgesellschaft mbH, within the research activities of the K2 Competence Centre on "Integrated Research in Materials, Processing and Product Engineering", operated by the Materials Center Leoben Forschung GmbH in the framework of the Austrian COMET Competence Centre Programme, is gratefully acknowledged.

References

[1] G. Jesner, S. Marsoner, I. Schemmel, K. Haeussler, R. Ebner, R. Pippan, Damage mechanisms in materials for cold forging dies under loading conditions typical for dies, International Journal of Microstructure and Materials Properties 3 (2-3) (2008) 297–310.
[2] T. Ø. Pedersen, Numerical modelling of cyclic plasticity and fatigue damage in cold-forging tools, International Journal of Mechanical Sciences 42 (4) (2000) 799 – 818.
[3] C. O. Frederick, P. J. Armstrong, A mathematical representation of the multiaxial bauschinger effect, Materials at High Temperatures 24 (1) (2007) 1–26.
[4] J. L. Chaboche, O. Jung, Application of a kinematic hardening viscoplasticity model with thresholds to the residual stress relaxation, International Journal of Plasticity 13 (10) (1997) 785–807.
[5] D. C. Drucker, Relations of experiments to mathematical theories of plasticity, Journal of Applied Mechanics 16 (1949) 349–357.
[6] J. P. Hirth, M. Cohen, On the strength-differential phenomenon in hardened steel, Metallurgical Transactions 1 (1) (1970) 3–8.
[7] W. C. Leslie, R. J. Sober, The strength of ferrite and of martensite as functions of compositions, temperature and strain rate, Trans. ASM 60 (3) (1967) 459.
[8] P. W. Bridgman, Studies in large plastic flow and fracture, with special emphasis on the effects of hydrostatic pressure, McGraw-Hill, 1952.
[9] S. K. Iyer, C. J. Lissenden, Multiaxial constitutive model accounting for the strength-differential in inconel 718, International Journal of Plasticity 19 (12) (2003) 2055 – 2081, special Issue in Honour of Professor Zenon Mroz.
[10] E. Patoor, M. El Amrani, A. Eberhardt, M. Berveiller, Determination of the origin for the dissymmetry observed between tensile and compression tests on shape memory alloys, Journal de Physique IV 5 (1995) 495–500, colloque C2, supplément au Journal de Physique III.
[11] S. Iyer, Viscoplastic model development to account for strength differential: Application to aged inconel 718 at elevated temperature, Tech. rep., Pennsylvania State University (2000).
[12] J. L. Chaboche, On some modifications of kinematic hardening to improve the description of ratchetting effects, International Journal of Plasticity 7 (7) (1991) 661–678.
[13] J. Besson, R. Foerch, Large scale object-oriented finite element code design, Computer Methods in Applied Mechanics and Engineering 142 (1-2) (1997) 165 – 187.
[14] Abaqus Theory Manual – Version 6.10, USA (2010).
[15] E. Doege, H. Meyer-Nolkemper, I. Saeed, Fließkurvenatlas metallischer Werkstoffe. mit Fließkurven für 73 Werkstoffe u. e. grundlegenden Einführung, Hanser, München u.a., 1986.